
Research Paper

Complement Activation by Core–Shell Poly(isobutylcyanoacrylate)–Polysaccharide Nanoparticles: Influences of Surface Morphology, Length, and Type of Polysaccharide

Isabelle Bertholon,¹ Christine Vauthier,¹ and Denis Labarre^{1,2}

Received October 27, 2005; accepted January 24, 2006

Purpose. Biodistribution of intravenously administered nanoparticles depends on opsonization. The aim of this study was the evaluation of complement activation induced by nanoparticles coated with different polysaccharides. Influences of size and configuration of dextran, dextran sulfate, or chitosan bound onto nanoparticles were investigated.

Method. Core–shell nanoparticles were prepared by redox radical or anionic polymerization of isobutylcyanoacrylate in the presence of polysaccharides. Conversion of C3 into C3b in serum incubated with nanoparticles was evaluated.

Results. Cleavage of C3 increased with size of dextran bound in “loops” configuration, whereas it decreased when dextran was bound in “brush.” It was explained by an increasing steric repulsive effect of the brush, inducing poor accessibility to OH groups. The same trend was observed for chitosan-coated nanoparticles. Nanoparticles coated with a brush of chitosan activated the complement system lesser than nanoparticles coated with a brush of dextran. This was explained by an improved repelling effect. Dextran-sulfate-coated nanoparticles induced a low cleavage of C3 whereas it strongly enhanced protein adsorption.

Conclusion. Complement activation was highly sensitive to surface features of the nanoparticles. Type of polysaccharide, configuration on the surface, and accessibility to reactive functions along chains are critical parameters for complement activation.

KEY WORDS: complement activation; core–shell nanoparticles; poly(isobutylcyanoacrylate); polysaccharide; surface properties.

INTRODUCTION

Many types of nanoparticles have been developed for drug delivery, but the fate of these systems after intravenous administration was usually not fully controlled. Thus, understanding the relationships between the properties of nanoparticles and their *in vivo* biodistribution has been an active field of investigation. Several authors reported that the fate of nanoparticles depended greatly on their surface properties' changing the interactions with serum proteins (1–9). Protein deposition and nonspecific recognition, i.e., opsonization, of nanoparticles as foreign bodies led usually to a short blood lifetime and fast accumulation in organs of the mononuclear phagocyte system, including the liver and the spleen (10). The complement system and especially protein C3 are strongly involved in the opsonization process (11).

The most common strategy to increase the blood circulation time of colloidal drug delivery systems is to coat their surface with poly(ethylene oxide) (PEO), inducing a steric repulsive effect toward protein adsorption. For instance, this can be achieved by preparing amphiphilic block copolymers containing at least one block of PEO. Then, by tailoring the copolymer in such a way that it may self-organize as core–shell nanoparticles when it is dispersed in aqueous solution, long circulating nanoparticles can be prepared (12). Concerning nanoparticles coated with PEO, the important parameters resulting in long circulation through steric repulsion have been shown to be the density, the length, and the conformation of the PEO chains on the nanoparticle surface (6,13–15).

Core–shell nanoparticles could be prepared from various amphiphilic copolymers, including those containing poly(alkylcyanoacrylate) (PACA). The first biodegradable nanoparticles obtained with PACA by Couvreur *et al.* (16) were prepared by anionic emulsion polymerization (AEP-pH 2.5) of alkylcyanoacrylate (ACA) in the presence of dextran. They were reported to accumulate massively in liver and spleen a few minutes after intravenous administration (10,16,17). The biodistribution of PACA nanoparticles could be modulated by binding PEO on the surface (18,19).

¹Laboratoire de Physico-chimie, Biopharmacie, Pharmacotechnie, UMR CNRS 8612, Faculté de Pharmacie, 5 rue Jean-Baptiste Clément, 92296 Châtenay-Malabry, Cedex, France.

²To whom correspondence should be addressed. (e-mail: denis.labarre@cep.u-psud.fr)

Other hydrophilic polymers have been proposed as steric repulsive agents. For instance, the effects of dextran coatings in end-on or side-on configurations toward adsorption of fibrinogen were compared with PEO by Österberg *et al.* (20). Side-on dextran was found to be as effective as end-on PEO in preventing fibrinogen adsorption. However, the effects toward other blood proteins and especially complement were not tested yet. Polysaccharides have a high potential as constituents of drug delivery systems. Some of them can be used as active agents, whereas others may be of interest in modifying the surface properties of nanoparticles and in preparing core-shell nanoparticles. In the latter case, testing the interactions between polysaccharide-coated nanoparticles and complement is of prime importance. Indeed, whereas complement is generally not activated by soluble polysaccharides, the immobilization of the polysaccharide on a surface endowed the resulting surface with complement-activating properties, increasing in turn the probability of a strong interaction with phagocytes. When the coating-surface-activating complement is on nanoparticles, the nanoparticles are quickly endocytosed by phagocytes. Although the mechanisms of complement activation by polysaccharide-coated surfaces are not fully understood, it is clear that a strong activation can be induced by reaction of the active form of C3 with nucleophilic groups present on a surface in contact with serum in the presence of divalent ions (21). However, it also appears that the activation depends on the conformation of the polysaccharide chains arranged at the surface of polymer particles. Indeed, the capacity of bound dextran to activate complement tested with cross-linked dextran particles, *i.e.*, Sephadex[®], showed a strong activation (22), whereas nonbiodegradable nanoparticles coated with a dextran "brush" only showed a weak activation of complement *in vitro* (9). After intravenous administration to mice, these particles remained in the bloodstream longer than corresponding uncoated systems (8).

In previous works (23,24), we showed that the activation of complement induced by dextran-coated biodegradable nanoparticles may depend on the method of preparation of the nanoparticles, which affected the conformation of the dextran chains at the nanoparticle surface. To better understand this effect, the aim of this study was to examine the activation of the complement system produced by a series of core-shell nanoparticles prepared from different types of polysaccharides having different molecular weights and different surface morphologies. The nanoparticle core was made of poly(isobutylcyanoacrylate) (PIBCA), and the shell was composed of either dextran, dextran sulfate, or chitosan. The nanoparticles were prepared by two emulsion polymerizations of isobutylcyanoacrylate (IBCA) in aqueous medium. The polymerization was initiated on the polysaccharide either through anionic (AEP-pH 2.5) or redox radical emulsion polymerization (RREP) mechanisms (25). As assumed in previous papers (24), AEP-pH 2.5 led to the formation of branched copolymers with a polysaccharide backbone and PIBCA side chains. These copolymers self-associate into nanoparticles with polysaccharide chains arranged in "loops and trains," or side-on, at the nanoparticle surface. In the case of the RREP, radicals are created at the end of the polysaccharide chain after reaction with cerium (IV) ions at pH 1, leading to the formation of block copol-

ymers. These copolymers self-associated into nanoparticles, with the polysaccharide attached by only one point on the PIBCA core surface. The polysaccharide chains are arranged as a brush, or end-on, at the nanoparticle surface. For the first time, this study investigates in detail the incidence of the polysaccharide-coating properties of biodegradable nanoparticles on the complement activation induced by those nanoparticles. It is expected that the results of this study will impact the design of nanoparticles for intravenous delivery of drugs in the future.

MATERIALS AND METHODS

Materials

Isobutylcyanoacrylate, kindly provided as a gift by Loctite (Dublin, Ireland), was used as monomer. Dextran (10, 66.9, 71, and 73.2 kDa) and dextran sulfate (10 and 500 kDa) were purchased from Sigma (Saint-Quentin Fallavier, France). Dextran (1.5, 15–20, 40, 60, and 100 kDa), dextran sulfate (5 kDa), and chitosan (medium molecular weight) were purchased from Fluka (Saint-Quentin Fallavier, France), and dextran sulfate (36–50 kDa) was supplied by ICN Biomedicals (Orsay, France). Cerium (IV) ammonium nitrate, nitric acid, and trisodium citrate dihydrate were purchased from Fluka. Polyclonal antibody to human C3 was purchased from Sigma. Other chemicals were of reagent grade and used as purchased.

Preparation of Chitosan of Various Molecular Weights

Depolymerization of Chitosan

Chitosan was selectively depolymerized by reaction with sodium nitrite at various concentrations (26). Typically, a chitosan solution (100 mL, 2% w/v) in acetic acid (6% v/v) reacted for 1 h at room temperature and under magnetic stirring with 10 mL of sodium nitrite, in a range of concentration between 15 and 89 mmol/L. Chitosan was precipitated by raising the pH to 9 with sodium hydroxide. The precipitate was recovered by filtration and washed extensively with acetone before it was dried. Chitosan dissolved in 0.1 M acetic acid was further purified by dialysis against water for 24 h. The prepared solutions were freeze dried before storage.

Measurement of Molecular Weight

The molecular weight of chitosan was determined by capillary viscosity measurements. Briefly, the reduced viscosity of chitosan solutions of various concentrations (0.1 to 2.5 g/L) in 0.1 M acetic acid and 0.2 M NaCl was measured in a Ubbelohde tube (53710/1 Schott Geräte) at 25°C (Bath CT1450 Schott Geräte and cooling system CK100 Schott Geräte) using a viscometer AVS400 (Schott Geräte). The intrinsic viscosity (η) was then deduced from the reduced viscosity measured for each solution of chitosan by extrapolation at zero concentration. The molecular weight was determined by using the Mark Houwink Sakurada equation: (η) = $K \times M^a$, with $K = 1.81 \times 10^{-3}$ and $a = 0.93$ (27).

Determination of Deacetylation Degree

Deacetylation degree was calculated from nuclear magnetic resonance (NMR) spectra obtained in D₂O/CD₃COOD according to Hirai *et al.* (28).

$$\text{Deacetylation degree(\%)} = (1 - (1/3 \times I_{\text{CH}_3}/1/6 I_{\text{H}_2-\text{H}_6})) \times 100$$

where I_{CH_3} is the intensity of proton of acetyl group at 2 ppm and $I_{\text{H}_2-\text{H}_6}$ is the intensity of signals of protons of glucose ring at 3.7–4 ppm.

Polymerization Procedure

Redox Radical Emulsion Polymerization

Redox radical emulsion polymerization was carried out according to the method described by Chauvierre *et al.* (25). A polysaccharide (dextran, dextran sulfate, or chitosan; 0.1375 g) was dissolved in 8 mL of aqueous 0.2 M nitric acid in a glass tube at 40°C under gentle stirring and argon bubbling. After 10 min, 2 mL of a solution of 8×10^{-2} M cerium (IV) ammonium nitrate in 0.2 M nitric acid was added. Then, IBCA (0.5 mL) was immediately added under stirring, which was vigorous enough to create a vortex. Argon bubbling was maintained for 10 min. The reaction was left to continue under gentle stirring for 50 min. After cooling down to room temperature and in the cases of polymerizations performed with dextran or dextran sulfate, 1.25 mL of an aqueous solution of 1 M trisodium citrate dihydrate was added. The pH of all the preparations was adjusted to 7.0 with 1 M aqueous NaOH. A milky suspension of polymeric particles was obtained.

AEP-pH 2.5

The anionic emulsion polymerization was performed according to the procedure described by Couvreur *et al.* (16). Dextran (0.05 g) was dissolved in 10 mL of aqueous 3×10^{-3} M hydrochloric acid at room temperature. Then, 100 μ L of IBCA was added dropwise under vigorous stirring. After 3 h, the pH was adjusted to 7.0 with 1 M aqueous NaOH. A milky suspension of polymeric particles was obtained.

AEP-pH 1

In the presence of chitosan, anionic polymerization was performed at pH 1 in 0.2 M nitric acid. The procedure was identical to that one described for RREP but without cerium and argon bubbling. Briefly, chitosan (0.1375 g) was dissolved in 8 mL of 0.2 M nitric acid at 40°C and under magnetic stirring. After total dissolution, IBCA (0.5 mL) was added under agitation, which was vigorous enough to create a vortex. The reaction was left to continue under magnetic stirring for 1 h. After cooling down to room temperature, the pH of the preparations was adjusted to 7.0 with 1 M aqueous NaOH. A milky suspension of nanoparticles was obtained.

Purification of Nanoparticles

The polymer suspensions prepared from the different polymerizations were purified by dialysis (Spectra/Por[®] membrane, molecular weight cutoff 100,000 Da; Biovalley, Marne la Vallée, France) twice against 1 L of distilled water for 90 min and once overnight. The purified suspensions were stored at 4°C until use.

Freeze Drying

The suspensions were frozen at -18°C and freeze dried during 48 h (Christ Alpha 1–4 freeze dryer, Bioblock Scientific, Illkirch, France) without the use of a cryoprotecting agent.

Nanoparticle Characterization

Particle Size

The hydrodynamic diameter of the nanoparticles was measured at 20°C via quasielastic light scattering using a Nanosizer N4 PLUS (Beckman-Coulter, Villepinte, France) operating at 90°. The samples were diluted in MilliQ[®] water by 1:300 (v/v) for nanoparticles made via RREP and by 1:150 (v/v) for nanoparticles formed via AEP-pH 2.5. Measurements of the hydrodynamic diameter at various temperatures were performed after 10 min of equilibration.

The results were expressed as the average of the mean hydrodynamic diameter of the dispersed particles obtained from three determinations. The standard deviation of the size distribution and the polydispersity index were also given. The polydispersity index given by the apparatus is equivalent to the variance of the lognormal distribution. The dispersion was considered as monodisperse when the polydispersity index was lower than 0.1.

Zeta Potential

The electrostatic surface charge of the polymer particles was determined from the electrophoretic mobility using a Zetasizer 4 (Malvern Instruments Ltd., Orsay, France). Dilution of the suspensions [1:200 (v/v)] was performed in 1 mM NaCl.

Morphology of Nanoparticles

The morphology of the nanoparticles was observed by scanning electron microscopy (SEM; LEO 9530, France) with a Gemini Column. The nanoparticles were freeze dried and then mounted on supports and coated with a Pt/Pd layer (Cressington, 208 HR) under an argon atmosphere.

Redispersion after Freeze Drying or Ultracentrifugation

The ability of the nanoparticle to be redispersed was tested after freeze drying and ultracentrifugation. The nanoparticles were ultracentrifuged (Optima LE 80K, Beckman Coulter, Villepinte, France) at 30,000 rpm for 30 min.

Redispersion in water after ultracentrifugation or freeze drying was obtained by using ultrasound bath and vortex.

Concentration of Nanoparticles

The nanoparticle suspensions were concentrated to obtain a surface of 2000 cm² in 200 μL for complement activation. Nanoparticles prepared via RREP were concentrated by freeze drying, and nanoparticles prepared via anionic polymerizations, i.e., AEP-pH 2.5 and AEP-pH 1, were ultracentrifuged (Optima LE 80K, Beckman Coulter) at 30,000 rpm for 30 min. Thereafter, the concentration of the suspensions was adjusted with the addition of ultrapure water (MilliQ®).

Evaluation of Complement Activation by 2-D Immunoelectrophoresis of C3

Protein C3 is a major plasma protein of the complement system circulating in functionally inactive form and is involved in the nonspecific recognition, i.e., opsonization, of foreign bodies. A critical step of complement activation consists in the cleavage of C3 into a large fragment, C3b, and a small fragment, C3a. Functionality of complement needs the presence of divalent ions. Thus, complement activation is assessed in human serum.

The complement activation of different nanoparticles was determined by studying the conversion of C3 into C3b by 2-D immunoelectrophoresis using a polyclonal antibody to human C3, according to the method of Laurell (29). Human serum was obtained after calcifying plasma from healthy donors and stored at -80°C until use. Veronal-buffered saline (VBS), VBS containing 0.15 mM Ca²⁺ and 0.5 mM Mg²⁺ ions (VBS²⁺), and VBS containing 40 mM ethylenediaminetetraacetic acid (VBS-EDTA) were prepared as described previously by Kazatchkine *et al.* (30). Nanoparticle suspensions (200 μL) were incubated under gentle agitation for 1 h at 37°C with 100 μL human serum and 100 μL VBS²⁺. To ensure a valid comparison of the different nanoparticles, the 200-μL sample volume of nanoparticles contained an equal surface area of hydrated particles corresponding to 2000 cm², calculated from the average hydrodynamic diameters according to Vittaz *et al.* (13).

After incubation, 5 μL of each sample was subjected to a first electrofocusing electrophoresis on 1% agarose gel. The 2-D electrophoresis was carried out on Gelbond® films in agarose gel plates containing a polyclonal antibody to human C3 (complement C3 antiserum rose in goat; Sigma, Lyon, France), recognizing both C3 and C3b. The films were finally stained with Coomassie blue to reveal the presence of C3 and C3b, which have reacted with the antibody (Sigma, Lyon, France). Serum diluted in VBS-EDTA (1:4 v/v) was used as negative control of complement activation. Serum diluted in VBS²⁺ was used as control of the spontaneous activation of complement occurring in the experimental conditions used. Sephadex® G 25 superfine (Pharmacia, Orsay, France), incubated in serum diluted in VBS²⁺, was used as a positive control. Each sample of nanoparticles was analyzed three times across the whole process. The height of the peaks, shown on the immunoelectrophoretic plate, corresponding to C3 and C3b, respectively, was measured. The activation of complement was expressed as the ratio of the peak height of C3b detected on the plate regarding the sum of the peak heights of C3 and C3b (C3b/(C3 + C3b)). In serum diluted in

VBS-EDTA, the ratio was equal to zero. In the presence of nanoparticles incubated with serum diluted in VBS²⁺, an increase of the ratio meant that the activating capacity of the nanoparticles increased.

RESULTS

Influence of the Method of Polymerization on Nanoparticle Characteristics

Nanoparticles of PIBCA coated with dextran were prepared from dextran of increasing molecular weight either via AEP-pH 2.5 according to Couvreur *et al.* (16) or via RREP according to Chauvierre *et al.* (25). Their hydrodynamic diameter is reported in Fig. 1A. When dextran of molecular weight lower than 6 kDa was used, polymeric particles of large diameter were formed and polydispersity index was high. The results were consistent with the fact that these suspensions also contained aggregates. Stable polymeric nanoparticle dispersions with well-defined diameters were prepared with dextran of higher molecular weight. For nanoparticles made via RREP, the diameter of the nanoparticles increased with molecular weight of the dextran chains higher than 10 kDa. For nanoparticles made via AEP-pH 2.5, the diameter was almost constant with the molecular weight of dextran. The difference in the relationships between the diameter of the nanoparticles and the molecular

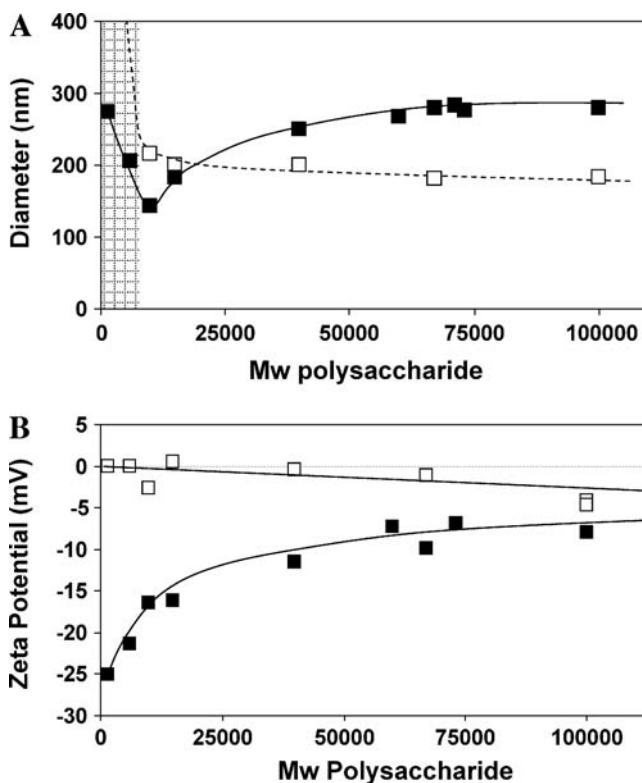


Fig. 1. Diameter (A) and zeta potential (B) of the nanoparticles produced via redox radical (filled symbols) and anionic (open symbols) emulsion polymerization. Hatched area: unstable polymeric particle suspensions.

weight of dextran for each type of polymerization could be explained by the different configurations of the dextran chains at the nanoparticle surface. It can be suggested that the dextran layer forming “loops and trains” on the surface of the nanoparticles made via AEP-pH 2.5 was more compact than the dextran layer arranged in brush at the surface of the nanoparticles made via RREP. Indeed, in this last configuration, dextran chains can be stretched and the thickness of the layer can increase with molecular weight as demonstrated by de Gennes (31).

As shown in Fig. 1B, differences on the nanoparticle characteristics due to the effects of the polymerization methods appeared more clearly considering the zeta potential of the nanoparticles. Indeed, the zeta potential of nanoparticles prepared via AEP-pH 2.5 was not affected by the molecular weight of dextran and remained close to neutrality. In contrast, the zeta potential of nanoparticles obtained via RREP increased with molecular weight of dextran to reach values close to neutrality for dextran of high molecular weight. The modification of the zeta potential observed for the nanoparticles obtained via RREP can be explained by the fact that the dextran layer that forms at the nanoparticle surface shields the negative charge of the nanoparticle PIBCA core and that the shield effect varies with the molecular weight of the dextran chains forming the polysaccharide brush at the nanoparticle surface. According to the results, it clearly appeared that the shield effect

produced by the dextran chains, arranged as loops and trains at the surface of the nanoparticles obtained via AEP-pH 2.5, was more efficient than the effect obtained by the dextran chains arranged as a brush at the surface of the nanoparticles prepared via RREP.

The aforementioned results are consistent with the hypothesis that the outermost structure of the nanoparticles obtained via AEP-pH 2.5 in the loops-and-trains structure was more compact than the brush structure of the nanoparticles obtained via RREP.

Freeze-dried samples of nanoparticles obtained by using both methods were observed via SEM (Fig. 2). At high magnification, individual nanoparticles were clearly observed from freeze-dried samples of the nanoparticles prepared via RREP. In contrast, freeze-dried nanoparticles obtained from AEP-pH 2.5 strongly adhered to each other, appearing as soft spheres. The different morphologies of the powders may be due to differences in surface properties of the nanoparticles, depending on the method of synthesis that affected the interactions between nanoparticles during the freeze-drying process.

Differences in the surface properties of the nanoparticles were also highlighted by investigating the redispersion of the nanoparticles into aqueous suspensions after either freeze drying or ultracentrifugation. After freeze drying, the diameter of the nanoparticles prepared via RREP could be recovered, indicating that these nanoparticles could be

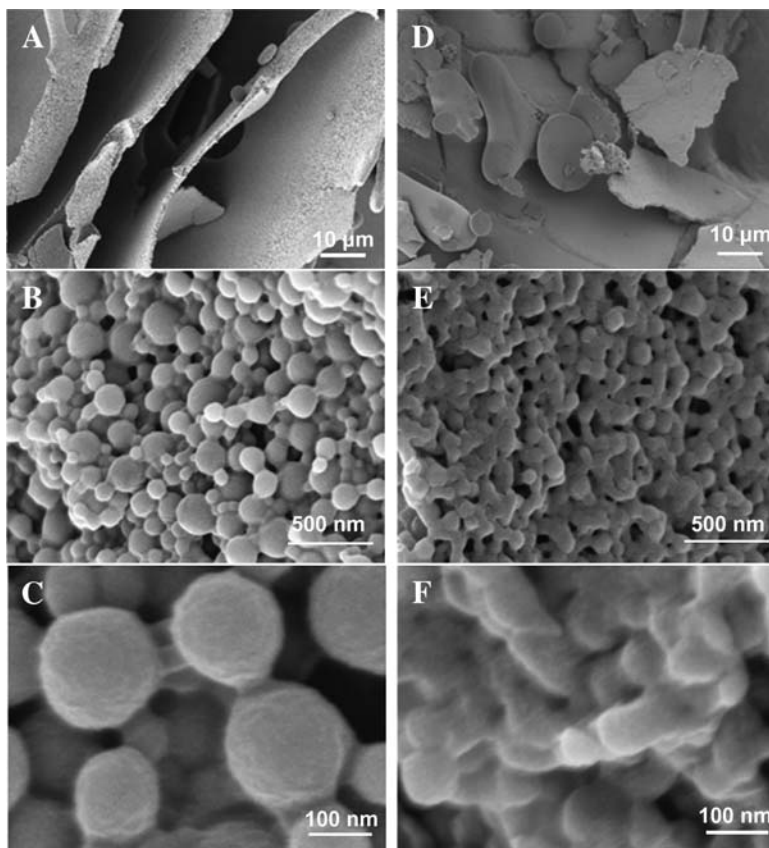


Fig. 2. Scanning electron micrographs at different magnifications of nanoparticles prepared with 66.9 kDa dextran via redox radical (A, B, C) and anionic (D, E, F) emulsion polymerizations after freeze drying.

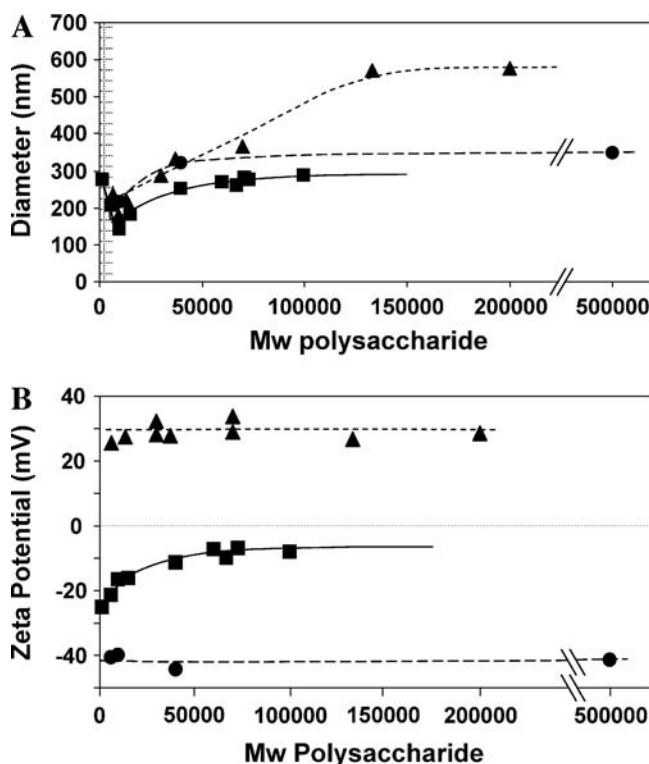


Fig. 3. Effect of the nature of the polysaccharide on the size (A) and zeta potential (B) of nanoparticle suspensions prepared via redox radical emulsion polymerization. The polysaccharides used were dextran (squares), chitosan (triangles), and dextran sulfate (circles).

completely redispersed. This was in agreement with the SEM observations of well-individualized nanoparticles. However, the pellet recovered from the ultracentrifugation of this nanoparticle suspension could not be redispersed, as shown by the presence of remaining aggregates even after redispersion with ultrasounds. Opposite results were obtained from redispersion assays of either freeze-dried nanoparticles prepared via AEP-pH 2.5 or pellet obtained from ultracentrifugation of these nanoparticles.

Influence of Type of Polysaccharide on Nanoparticle Characteristics

To further investigate the influences of both the nature and the configuration of the polysaccharide layer at the nanoparticle surface, we attempted to prepare nanoparticles coated with either dextran sulfate or chitosan by redox radical and anionic polymerization. At neutral pH, these polysaccharides are negatively charged (dextran sulfate, $pK_a < 2$) and at least partially positively charged (chitosan, $pK_a \sim 6.2$). Polymerization was initiated on polysaccharides of various molecular weights, and nanoparticles coated with either chitosan or dextran sulfate could be obtained via RREP. Nanoparticles coated with chitosan could also be obtained via anionic polymerization of IBCA in the presence of chitosan at pH 1 and in the absence of cerium (IV) ions (AEP-pH 1). This type of polymerization performed in the presence of dextran sulfate did not lead to nanoparticles but to the formation of a bulk precipitate. Diameter and zeta

potential of the nanoparticles, which could be obtained, were measured as depicted in Fig. 3. When nanoparticles were prepared via RREP, the diameter increased with the molecular weight of the polysaccharide, as observed in the case of dextran-bearing nanoparticles, but it was higher for the charged polysaccharides, especially chitosan. This is consistent with the electrostatic repulsion between the chains and with the higher persistence length of chitosan (5 nm in 0.2 M acetic acid, 0.15 M ammonium acetate) (32), when compared with the persistence lengths of dextran (1.8 nm in 0.1 M NaNO_3) (33) and dextran sulfate (1.6 nm in 0.1 M NaNO_3) (33). The zeta potential was not influenced by the molecular weight of charged polysaccharides and depended only on the polysaccharide used.

The diameter of the chitosan-coated nanoparticles synthesized by anionic polymerization at pH 1 was lower than the equivalent nanoparticles made via RREP, showing that the chitosan layer was more compact at the surface of the nanoparticles, as expected for a loops-and-trains configuration when compared with a brush configuration. Concerning zeta potential, surface charge of AEP-pH 1 chitosan nanoparticles was slightly higher when compared with RREP nanoparticles. It can be suggested that the chitosan layer was more compact at the surface of these nanoparticles and formed a more efficient shield to the contribution of the negative charge of the nanoparticle core to the zeta potential value (Table I).

Influence of the Structure of the Dextran Shell on the Activation of Complement

Complement activation was assessed in the presence of suspensions of dextran-bearing nanoparticles incubated in human serum diluted in VBS^{2+} for 1 h at 37°C. The amount of nanoparticles in contact with serum was adjusted to obtain equivalent contact surface areas. Cleavage of protein C3 was evidenced by 2-D immunoelectrophoresis, and the height of the peaks corresponding to C3 and C3b was measured (Fig. 4). Activation of complement was expressed as the ratio of the height of the C3b peak to the sum of the heights of the C3 and C3b peaks. The ratio was plotted vs. the molecular weight of dextran used in preparing the nanoparticles, and the results are shown in Fig. 5. In the presence of the nanoparticles made from 10 kDa dextran via RREP, about half of C3 present in serum was activated. Activation still decreased slowly even if molecular weight of dextran is increased. About 25% of C3 was activated in the presence of the nanoparticles made from 100 kDa dextran. When the molecular weight of dextran used in preparing nanoparticles was below 20 kDa, activation of C3 in the presence of similar

Table I. Characteristics of Nanoparticles Coated with Chitosan Obtained via AEP-pH 1

	Chitosan (30,000 g/mol)	Chitosan (70,000 g/mol)
Diameter (nm)	210 ± 21	250 ± 25
Polydispersity index	0.2	0.3
Zeta potential (mV)	32.3 ± 0.5	33.8 ± 0.5

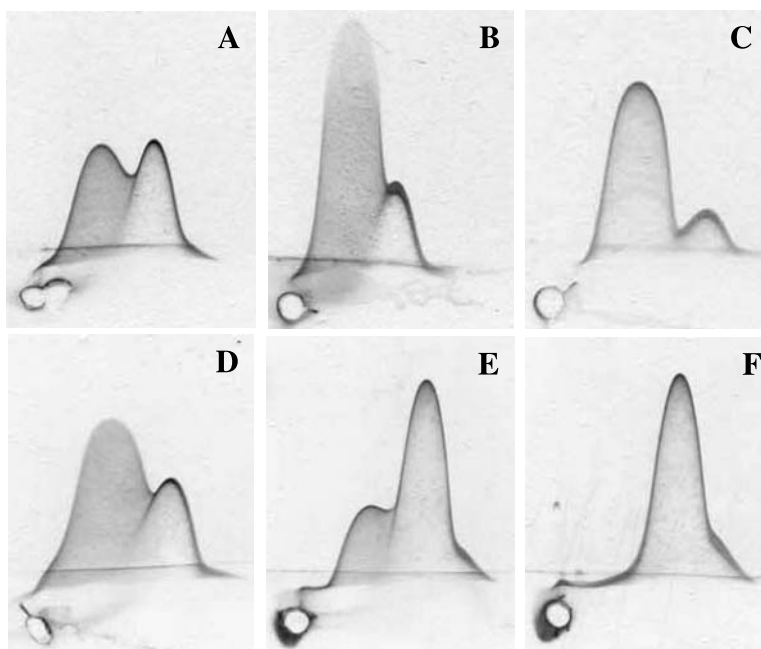


Fig. 4. Profile of complement activation for nanoparticles prepared via RREP (A, B, C) or AEP-pH 2.5 (D, E, F) from 10 kDa dextran (A, D), 67 kDa dextran (B, E), or 100 kDa dextran (C, F).

surface areas of the nanoparticles made via either AEP-pH 2.5 or RREP was in the same range. However, contrary to what was observed in the case of nanoparticles made via RREP, C3 activation increased with increasing molecular weight of dextran when the nanoparticles were prepared via AEP-pH 2.5. Protein C3 was even fully activated in the presence of the nanoparticles made from 100 kDa dextran. It can be noticed that the size of nanoparticles was not a relevant parameter to modulate complement activation because no correlation can be established between the level of complement activation measured and the size of the nanoparticles.

Influence of the Type of Polysaccharidic Shell on the Activation of Complement

To investigate the influence of the nature of the polysaccharide layer on nanoparticles, complement activation experiments were performed in the presence of nanoparticles coated with chitosan or dextran sulfate and obtained via RREP. Differences in complement activation were observed as a function of the nature of the polysaccharide. In the presence of 2000 cm² surface area of nanoparticles prepared with dextran sulfate, a high adsorption of proteins leading to aggregation of the sample was observed regardless of the molecular weight of dextran sulfate. In the case of nanoparticles prepared with dextran sulfate of low molecular weight (10 kDa), a small peak corresponding to C3 was found in the serum supernatant (Fig. 6). For nanoparticles made with dextran sulfate of medium molecular weight (35–50 kDa), a peak corresponding to C3 was detected only when the surface area of nanoparticles in contact with serum was decreased by at least four times. A small peak corresponding

to C3b or to further degraded fragments was also detected. It can be concluded from these results that nanoparticles prepared with dextran sulfate via RREP were weak complement activators but adsorbed a large amount of proteins, which led to aggregation. This high-protein adsorption is in agreement with previous works of different authors considering surfaces bearing sulfate groups (34–36).

In the presence of 2000 cm² surface area of the nanoparticles prepared via RREP with a 6-kDa chitosan, about half of C3 present in serum was activated. Increasing molecular weight of chitosan led to a strong decrease of complement activation (Figs. 7 and 8). The level of spontaneous activation was reached for nanoparticles prepared with chitosan above 70 kDa. When compared to nanoparticles prepared via RREP with dextran in a similar range

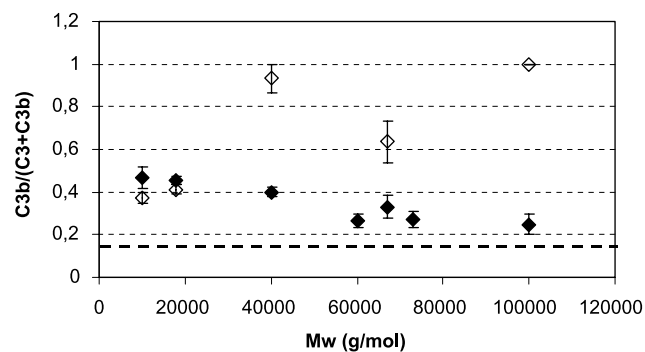


Fig. 5. Evolution of the ratio C3b/(C3 + C3b) as a function of the dextran molecular weight for nanoparticles obtained via RREP (filled diamond) and AEP-pH 2.5 (open diamond); spontaneous activation of the serum (black dashed line).

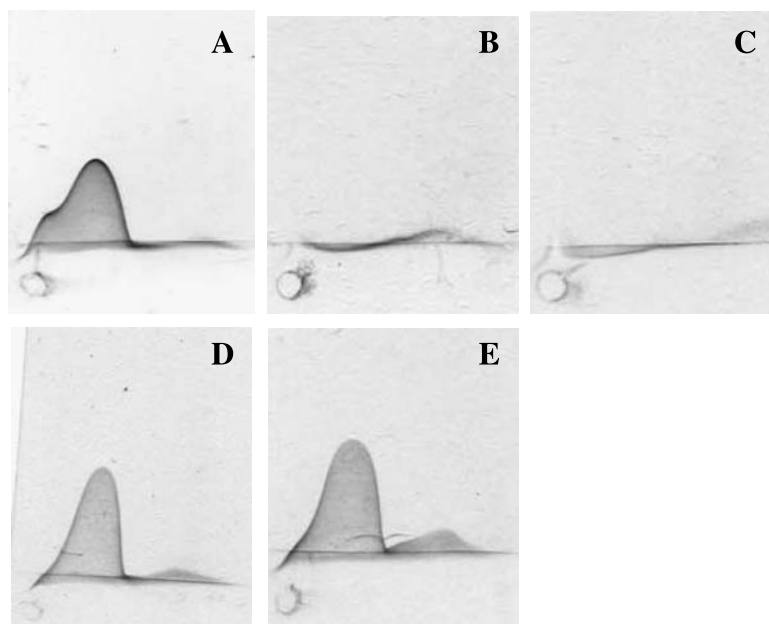


Fig. 6. Profile of complement activation for nanoparticles prepared with dextran sulfate via RREP with different molecular weights [10 kDa (A), 35–50 kDa (B, D, E), 500 kDa (C)] and different contact surfaces [2000 cm² (A, B, C), 500 cm² (D), 200 cm² (E)].

of molecular weight, nanoparticles coated with chitosan appeared as weaker activators of the complement system.

As it was not possible to prepare nanoparticles from dextran sulfate by anionic polymerization at pH 1, the influence of configuration of charged polysaccharide on complement activation could be tested only in the case of chitosan. Complement activation measured in the presence of nanoparticles prepared with chitosan at 30 and 70 kDa by anionic polymerization was markedly higher than complement activation measured with nanoparticles prepared via RREP with the same chitosans. However, it was lower than the activation measured in the presence of nanoparticles prepared via anionic polymerization with dextran in a similar

range of molecular weight (Figs. 6 and 8). From our results, neither the size of chitosan-coated nanoparticles nor the degree of deacetylation of chitosan within the range of 35–60% affected clearly the level of complement activation produced by the corresponding nanoparticles.

DISCUSSION

Influences of Method of Polymerization and Type of Polysaccharide on Nanoparticle Characteristics

The results obtained regarding size and zeta potential determinations are consistent with the assumption that the

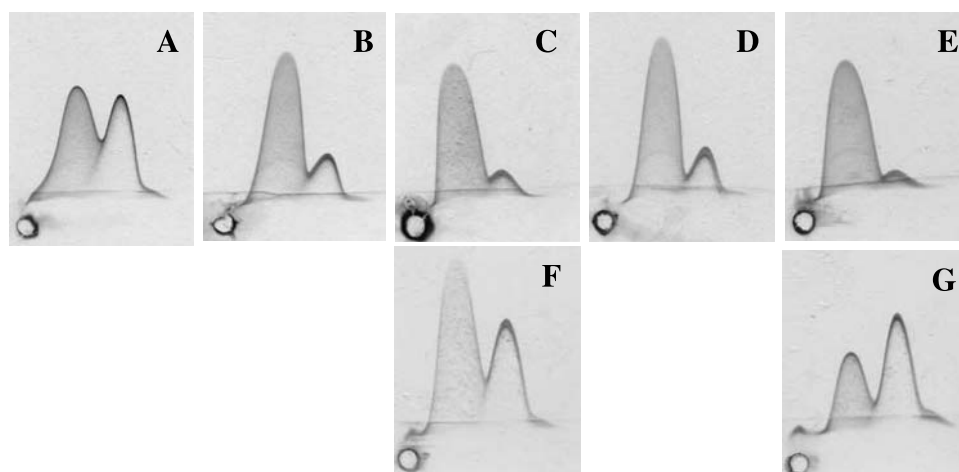


Fig. 7. Profile of complement activation for nanoparticles prepared with chitosan via RREP (A–E) or AEP-pH 1 (F, G) with different molecular weights: 6000 g/mol (A), 13,000 g/mol (B), 30,000 g/mol (C, F), 36,000 g/mol (D), 70,000 g/mol (E, G).

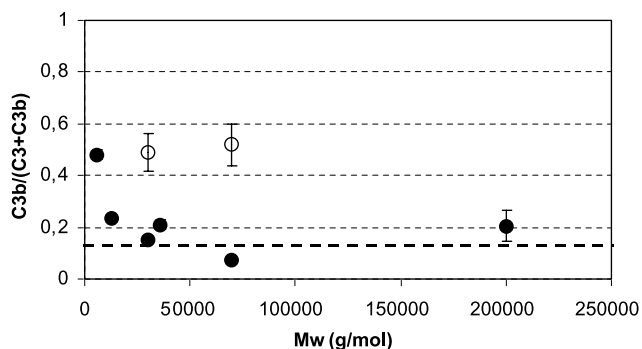


Fig. 8. Evolution of the ratio $C3b/(C3 + C3b)$ as a function of the chitosan molecular weight for nanoparticles obtained via RREP (filled circle) and AEP-pH 1 (open circle); spontaneous activation of the serum (black dashed line).

coating on the nanoparticles was in a brush configuration when prepared through redox radical polymerization of IBCA initiated by cerium (IV) in the presence of dextran, chitosan, or dextran sulfate. Size of the nanoparticles directly depended on size and charge of polysaccharide used in preparing them. Similarly, results obtained with nanoparticles prepared through an anionic polymerization of IBCA initiated in the presence of either dextran or chitosan are consistent with the assumption that the coating was in a more compact loops-and-trains configuration. The influence of the different surface morphologies on stability of dextran-coated nanoparticle suspensions was already obvious when concentrating them either by freeze drying or by ultracentrifugation.

Influence of Dextran Configuration on Complement Activation Induced by the Nanoparticles

Our results showed that complement activation was in the same range for nanoparticles prepared either via RREP or AEP-pH 2.5 with dextran of molecular weight lower than 20 kDa. This can be explained by the combined effects of the low efficiency of the short brush of dextran to cover the PIBCA core of the nanoparticles, as suggested by the zeta potential measurements, and by the availability of the OH functions of the dextran loops and trains arranged at the surface of nanoparticles prepared via AEP-pH 2.5 (21). The opposite effects observed when increasing the molecular weight of dextran can be explained by an increase in the thickness of the brush of the nanoparticles prepared via RREP, which led to an improved steric barrier against protein adsorption at the surface of the nanoparticles. In addition, it can be suggested that the OH groups of the dextran chains located inside the brush were less available for reaction with complement proteins, reducing capacity of the brush to induce complement activation. In the case of the nanoparticles prepared via AEP-pH 2.5, diameter and zeta potential of the nanoparticles remained constant despite the increase in the molecular weight of dextran, indicating that thickness of the dextran shell in loops and trains was not increased. Thus, the repelling effect was probably not improved, whereas the availability of the OH groups of dextran increased with "loops" length, leading to higher activation of complement. These results obtained from nanoparticles coated with dextran in two different config-

urations can be compared with the results published on surfaces bearing poly(ethylene glycol) (PEG) chains bound either end-on, i.e., brush, or side-on, i.e., loops and trains. Above 5 kDa, end-on bound PEG was highly efficient for repelling proteins, and increasing the molecular weight did not result in an increasing repelling effect (6,20). A dense brush of 2 kDa PEG was also sufficient to repel complement proteins (13). Compared to the fact that a minimal molecular weight of 10,000 g/mol was necessary to reduce complement activation with end-on bound dextran, end-on PEG is more efficient than dextran bound in a similar way for repelling proteins, including complement proteins. The apparent discrepancy with the results published by Österberg (20) concerning an efficient steric repulsion of fibrinogen by side-on dextran-coated surfaces can be easily explained by the absence of reactivity of fibrinogen toward OH-bearing surfaces. This is in contrast, considering that the proteins of complement, in which the major component, protein C3, strongly reacts with OH groups found on polymer surfaces, are responsible for the activation of the complement system. Our results emphasize the prime importance of the configuration of the dextran chains in the surface-coating layer to modulate the reaction of the OH groups with complement proteins. Thus, depending on this configuration, dextran chains with the same molecular weight and containing the same amount of OH groups may or may not induce complement activation. Such morphological differences may explain why some researchers working on complement activation induced by cellulose and regenerated cellulose membranes sometimes find inconsistent results.

Influence of Type of Polysaccharides

Concerning the possibility of using nanoparticles coated with dextran sulfate, results were clearly disappointing. It was not possible to obtain nanoparticles through anionic polymerization, at least in the conditions that were used in the present work. Nanoparticles could be obtained via RREP, but despite an apparently low complement-activating capacity, a very high adsorption of proteins leading to aggregation was observed. This strong protein adsorption on the nanoparticle surface hampered the use of the 2-D immunoelectrophoresis method to analyze complement activation produced by the corresponding nanoparticles.

The results obtained with chitosan-coated nanoparticles were rather unexpected. Indeed, the literature reporting interactions between chitosan and the complement system was not very clear. Chitosan was described as a complement activator. The complement activation was shown to increase with the number of NH_2 groups included along the chitosan chain (37,38). Other studies reported that chitosan-bearing surfaces exhibited an adsorption of proteins but no complement activation (39). In another way, chitin and chitosan were reported to activate the alternative complement pathway when they were bound on solid surfaces, but as water-soluble materials, they did not activate the complement system (39,40). After intravenous administration, chitosan-based nanoparticles were shown to avoid *in vivo* recognition by the mononuclear phagocyte system (41–43). In our experiments, complement activation by chitosan-coated nanoparticles clearly depended on configuration of chitosan

chains at the surface of nanoparticles in agreement with the results obtained with dextran-coated nanoparticles.

In the case of nanoparticles obtained via RREP, it can be assumed that chitosan chains present at the surface of the nanoparticles behaved like solubilized chitosan. Indeed, the diameter of the nanoparticles prepared via RREP continuously increased with the molecular weight of the chitosan, which indicated the presence of an extended hydrated layer of chitosan chains at the nanoparticle surface. Additionally, the nanoparticle suspensions were long-term stable (at least 2 years at neutral pH). Concerning complement activation, the deacetylation degree of chitosan was not an important parameter, at least in the range of 35–60% used in this study. As shown with dextran-coated nanoparticles, complement activation was also strongly influenced by molecular weight of chitosan and its configuration on the nanoparticle surface. However, a brush of chitosan obtained with polysaccharide chains with a molecular weight of more than 30 kDa was as efficient as a brush of 100-kDa dextran. The higher protection against complement activation observed with chitosan could be due either to an improved steric repulsion or to an inhibition of complement activation by chitosan. Some polyanions and polycations were described as inhibitors of complement (44,45), but this was not the case for chitosan, which was described to be an activator of the alternative pathway of complement (37,39,40). Thus, it appears that an improved steric repulsion, rather than an inhibition of complement, is more likely to explain the increased capacity to reduce complement activation by the chitosan brush at the nanoparticle surface. As highlighted by Österberg *et al.* (20), the great efficiency of surface-bound PEG in reducing protein adsorption is consistent with the large molecular exclusion volume due to a high hydration of this polymer. This has not been studied in the present work, but aqueous solutions of chitosan, which is a polyelectrolyte, are more viscous than solutions of dextran of the same molecular weight and at the same concentration, suggesting that chitosan has probably a higher hydrodynamic volume. Concerning steric repulsion of proteins, it means that protein adsorption should be more difficult on a chitosan layer than on a dextran layer of similar molecular weight and configuration.

CONCLUSION

In serum, the complement system is known to play a significant role in the nonspecific recognition of foreign bodies by the immune system of the organism. In the case of nanoparticles circulating in the bloodstream, a strong activation of complement generally results in extensive opsonization of the nanoparticle surface and fast uptake by activated phagocytes *in vivo*. In this article, the activation of complement was evaluated *in vitro* on a large series of nanoparticles composed of a PIBCA core and a polysaccharide shell showing various properties. Complement activation was shown to depend on the type of polysaccharide, length of the chain, and, overall, on the configuration of the polysaccharide chain on the nanoparticle surface. By increasing the length of side-on bound, i.e., loops and trains, dextran and chitosan resulted to an increase of complement activation. Conversely, by increasing the length of end-on bound, i.e., brush, dextran

and chitosan resulted to a decrease of complement activation; the effect was more pronounced with chitosan. These opposite effects were attributed to the combined effects of the repelling brush of the polysaccharide and to the availability of polysaccharide-reactive groups to the complement protein C3 in the loops-and-trains configuration of the polysaccharide chains. This work provides a clear understanding of the relationships between the complement activation produced by a series of polysaccharide-coated nanoparticles and properties of the nanoparticle surface. It may also clarify the contradictory results that were reported in the past in the literature. Relationships between complement activation and *in vivo* fate of the nanoparticles are currently investigated.

ACKNOWLEDGMENTS

The authors want to thank Dr. K. Broadley from Loctite (Dublin, Ireland) for his kindness in providing alkylcyanoacrylate monomer and Audrey Valette (CNRS-CEM Thiais) for the SEM. Isabelle Bertholon is a fellow of the Ministry of Research in France.

REFERENCES

1. S. Stolnik, B. Daudali, A. Arien, J. Whetstone, C. R. Heald, M. C. Garnett, S. S. Davis, and L. Illum. The effect of surface coverage and conformation of poly(ethylene oxide) (PEO) chains of poloxamer 407 on the biological fate of model colloidal drug carriers. *Biochim. Biophys. Acta, Biomembr.* **1514**:261–279 (2001).
2. H. Sahli, J. Tapon-Brethaudiere, A. M. Fischer, C. Sternberg, G. Spenlehauer, T. Verrecchia, and D. Labarre. Interactions of poly(lactic acid) and poly(lactic acid-co-ethylene oxide) nanoparticles with the plasma factors of the coagulation system. *Biomaterials* **18**:281–288 (1997).
3. J. Lee, P. A. Martic, and J. S. Tan. Protein adsorption on pluronic coated polystyrene particles. *J. Colloid Interface Sci.* **131**:252–266 (1989).
4. S. S. Davis, L. Illum, S. M. Moghimi, M. C. Davies, C. J. H. Porter, I. S. Muir, A. Brindley, N. M. Christy, M. E. Norman, P. Williams, and S. E. Dunn. Microspheres for targeting drugs to specific body sites. *J. Control. Release* **24**:157–163 (1993).
5. J. C. Neal, S. Stolnik, E. Schacht, E. R. Kenawy, M. C. Garnett, S. S. Davis, and L. Illum. *In vitro* displacement by rat serum of adsorbed radiolabeled poloxamer and poloxamine copolymers from model and biodegradable nanospheres. *J. Pharm. Sci.* **87**:1242–1248 (1998).
6. R. Gref, M. Luck, P. Quellec, M. Marchand, E. Dellacherie, S. Harnisch, T. Blunk, and R. H. Muller. 'Stealth' corona-core nanoparticles surface modified by polyethylene glycol (PEG): influences of the corona (PEG chain length and surface density) and of the core composition on phagocytic uptake and plasma protein adsorption. *Colloids Surf., B Biointerfaces* **18**:301–313 (2000).
7. D. Bazile, C. Prud'homme, M. T. Bassoulet, M. Marlard, G. Spenlehauer, and M. Veillard. Stealth Me.PEG-PLA nanoparticles avoid uptake by the mononuclear phagocytes system. *J. Pharm. Sci.* **84**:493–498 (1995).
8. C. Passirani, G. Barratt, J. P. Devissaguet, and D. Labarre. Long-circulating nanoparticles bearing heparin or dextran covalently bound to poly(methyl methacrylate). *Pharm. Res.* **15**:1046–1050 (1998).
9. C. Passirani, G. Barratt, J.-P. Devissaguet, and D. Labarre. Interactions of nanoparticles bearing heparin or dextran cova-

- lently bound to poly(methyl methacrylate) with the complement system. *Life Sci.* **62**:775–785 (1998).
10. V. Lenaerts, J. F. Nagelkerke, T. J. Van Berkel, P. Couvreur, L. Grislain, M. Roland, and P. Speiser. *In vivo* uptake of polyisobutyl cyanoacrylate nanoparticles by rat liver Kupffer, endothelial, and parenchymal cells. *J. Pharm. Sci.* **73**:980–982 (1984).
 11. M. D. Kazatchkine and M. P. Carreno. Activation of the complement system at the interface between blood and artificial surfaces. *Biomaterials* **9**:30–35 (1988).
 12. R. Gref, Y. Minamitake, M. T. Peracchia, V. Trubetskoy, V. Torchilin, and R. Langer. Biodegradable long-circulating polymeric nanospheres. *Science* **263**:1600–1603 (1994).
 13. M. Vittaz, D. Bazile, G. Spenlehauer, T. Verrecchia, M. Veillard, F. Puisieux, and D. Labarre. Effect of PEO surface density on long-circulating PLA–PEO nanoparticles which are very low complement activators. *Biomaterials* **17**:1575–1581 (1996).
 14. M. Malmsten, K. Emoto, and J. M. Van Alstine. Effect of chain density on inhibition of protein adsorption by poly(ethylene glycol) based coatings. *J. Colloid Interface Sci.* **202**:507–517 (1998).
 15. M. T. Peracchia, C. Vauthier, C. Passirani, P. Couvreur, and D. Labarre. Complement consumption by poly(ethylene glycol) in different conformations chemically coupled to poly(isobutyl 2-cyanoacrylate) nanoparticles. *Life Sci.* **61**:749–761 (1997).
 16. P. Couvreur, B. Kante, M. Roland, P. Guiot, P. Bauduin, and P. Speiser. Polycyanoacrylate nanocapsules as potential lysosomotropic carriers: preparation, morphological and sorptive properties. *J. Pharm. Pharmacol.* **31**:331–332 (1979).
 17. L. Grislain, P. Couvreur, V. Lenaerts, M. Roland, D. Deprez-Decampeneere, and P. Speiser. Pharmacokinetics and distribution of a biodegradable drug-carrier. *Int. J. Pharm.* **15**:335–345 (1983).
 18. M. T. Peracchia, E. Fattal, D. Desmaele, M. Besnard, J. P. Noel, J. M. Gomis, M. Appel, J. d'Angelo, and P. Couvreur. Stealth PEGylated polycyanoacrylate nanoparticles for intravenous administration and splenic targeting. *J. Control. Release* **60**:121–128 (1999).
 19. P. Calvo, B. Gouritin, H. Chacun, D. Desmaele, J. D'Angelo, J. P. Noel, D. Georgin, E. Fattal, J. P. Andreux, and P. Couvreur. Long-circulating PEGylated polycyanoacrylate nanoparticles as new drug carrier for brain delivery. *Pharm. Res.* **18**:1157–1166 (2001).
 20. E. Österberg, K. Bergström, T. P. Schuman, J. A. Riggs, N. L. Burn, J. M. Van Alstine, and J. M. Harris. Protein-rejection ability of surface-bound dextran in end-on and side-on configurations: comparison to PEG. *J. Biomed. Mater. Res.* **29**:741–747 (1995).
 21. S. K. Law, N. A. Lichtenberg, and R. P. Levine. Evidence for an ester linkage between the labile binding site of C3b and receptive surfaces. *J. Immunol.* **123**:1388–1394 (1979).
 22. M.-P. Carreno, D. Labarre, M. Jozefowicz, and M. D. Kazatchkine. The ability of Sephadex to activate human complement is suppressed in specifically substituted functional Sephadex derivatives. *Mol. Immunol.* **25**:165–171 (1988).
 23. C. Chauvierre, D. Labarre, P. Couvreur, and C. Vauthier. Novel polysaccharide-decorated poly(isobutyl cyanoacrylate) nanoparticles. *Pharm. Res.* **20**:1786–1793 (2003).
 24. I. Bertholon-Rajot, D. Labarre, and C. Vauthier. Influence of the initiator system, cerium-polysaccharide, on the surface properties of poly(isobutylcyanoacrylate) nanoparticles. *Polymer* **46**:1407–1415 (2005).
 25. C. Chauvierre, D. Labarre, P. Couvreur, and C. Vauthier. Radical emulsion polymerization of alkylcyanoacrylates initiated by the redox system dextran-cerium (IV) under acidic aqueous conditions. *Macromolecules* **36**:6018–6027 (2003).
 26. M. Huang, E. Khor, and L.-Y. Lim. Cellular uptake of chitosan—effect of the molecular weight. In c. r. society (ed.), *Winter Symposium & 11th International Symposium on Recent Advances in Drugs Delivery Systems*, Salt Lake City, Utah, USA, 2003, p. 119.
 27. T. Khan, K. Peh, and H. Ch'ng. Mechanical, bioadhesive strength and biological evaluations of chitosan films for wound dressing. *J. Pharm. Pharm. Sci.* **3**:303–311 (2000).
 28. A. Hirai, H. Odani, and A. Nakajima. Determination of degree of deacetylation of chitosan by ¹H NMR spectroscopy. *Polym. Bull.* **26**:87–94 (1991).
 29. C. B. Laurell. Quantitative estimation of proteins by electrophoresis in agarose gel containing antibodies. *Anal. Biochem.* **15**:45–52 (1966).
 30. M. D. Kazatchkine, G. Hauptmann, and U. E. Nydegger. *Technique du Complément*, INSERM, Paris, 1986, pp. 22–23.
 31. P. G. de Gennes. Conformation of polymers attached to an interface. *Macromolecules* **13**:1069–1075 (1980).
 32. C. Schatz, C. Viton, T. Delair, C. Pichot, and A. Domard. Typical physicochemical behavior of chitosan in aqueous solution. *Biomacromolecules* **4**:641–648 (2003).
 33. J. A. White and W. M. Deen. Agarose–dextran gels as synthetic analogs of glomerular basement membrane: water permeability. *Biophys. J.* **82**:2081–2089 (2002).
 34. D. Labarre, C. Vauthier, C. Chauvierre, B. Petri, R. Muller, and M. M. Chehimi. Interactions of blood proteins with poly(isobutylcyanoacrylate) nanoparticles decorated with a polysaccharidic brush. *Biomaterials* **26**:5075–5084 (2005).
 35. Y. Murakami, H. Iwata, E. Kitano, H. Kitamura, and Y. Ikada. Interaction of poly(2-acrylamido 2-methylpropane sulfonate)-grafted polystyrene beads with cationic complement proteins. *J. Biomater. Sci., Polym. Ed.* **12**:451–465 (2001).
 36. J. Janatova, A. K. Cheung, and C. J. Parker. Biomedical polymers differ in their capacity to activate complement. *Complement Inflamm.* **8**:61–69 (1991).
 37. Y. Suzuki, K. Miyatake, Y. Okamoto, E. Muraki, and S. Minami. Influence of the chain length of chitosan on complement activation. *Carbohydr. Polym.* **54**:465–469 (2003).
 38. S. Minami, H. Suzuki, Y. Okamoto, T. Fujinaga, and Y. Shigemasa. Chitin and chitosan activate complement via the alternative pathway. *Carbohydr. Polym.* **36**:151–155 (1998).
 39. J. Benesch and P. Tengvall. Blood protein adsorption onto chitosan. *Biomaterials* **23**:2561–2568 (2002).
 40. Y. Suzuki, Y. Okamoto, M. Morimoto, H. Sashiwa, H. Saimoto, S. I. Tanioka, Y. Shigemasa, and S. Minami. Influence of physico-chemical properties of chitin and chitosan on complement activation. *Carbohydr. Polym.* **42**:307–310 (2000).
 41. T. Banerjee, S. Mitra, A. Kumar Singh, R. Kumar Sharma, and A. Maitra. Preparation, characterization and biodistribution of ultrafine chitosan nanoparticles. *Int. J. Pharm.* **243**:93–105 (2002).
 42. T. Banerjee, A. K. Singh, R. K. Sharma, and A. N. Maitra. Labeling efficiency and biodistribution of Technetium-99m labeled nanoparticles: interference by colloidal tin oxide particles. *Int. J. Pharm.* **289**:189–195 (2005).
 43. Y. J. Son, J.-S. Jang, Y. W. Cho, H. Chung, R.-W. Park, I. C. Kwon, I.-S. Kim, J. Y. Park, S. B. Seo, C. R. Park, and S. Y. Jeong. Biodistribution and anti-tumor efficacy of doxorubicin loaded glycol-chitosan nanoaggregates by EPR effect. *J. Control. Release* **91**:135–145 (2003).
 44. F. Maillat and M. D. Kazatchkine. Modulation of the formation of the human amplification C3 convertase of complement by polycations. *Immunology* **50**:27–33 (1983).
 45. J. M. Weiler and R. J. Linhardt. Comparison of the activity of polyanions and polycations on the classical and alternative pathways of complement. *Immunopharmacology* **17**:65–72 (1989).